ERDC/CHL CHETN-III-79
January 2009

US Army Corps of Engineers®

Shear Stress Estimates for Combined Wave and Surge Overtopping at Earthen Levees

by Norberto C. Nadal and Steven A. Hughes

PURPOSE: The Coastal and Hydraulics Engineering Technical Note (CHETN) described herein provides empirical equations for estimating shear stresses on the land-side slope of earthen levees resulting from the combination of storm surge steady overflow and unsteady overtopping of irregular waves. A worked example provides guidance on application of the empirical equations.

INTRODUCTION AND BACKGROUND: Earthen levees are used extensively throughout the world to protect the population and infrastructure against flooding in low-lying developed areas. Ideally, all levees would have crown elevations with enough freeboard to prevent overtopping for any possible scenario, from periodic floods to high waters due to storm surges. However, economics often dictate that levees be designed with lower crown elevations that allow for an acceptable risk of overtopping during extreme storm events. Investigations performed after Hurricane Katrina revealed that most of the earthen levee damage occurred on the landward-side slopes by either: (a) wave-only overtopping when the water level was below the levee crest elevation, (b) storm surge overflow when the water level exceeded the crest elevation, or (c) a combination of both surge overflow and wave overtopping.

Overtopping of earthen levees produces fast, turbulent flow velocities on the landward-side slope that can damage the protective grass covering and expose the underlying soil to erosion. A rapid loss of unprotected soil during an overtopping event could lead to loss of levee crest elevation, and possibly breaching of the protective structure. Therefore, the crown and landward-side slopes of those levees that are at risk of overtopping must be protected with some type of strengthening method such as turf reinforcement, soil strengthening, or hard armoring. Assessment of levee reliability and design of slope protection alternatives requires knowledge of probable storm scenarios and estimates of flow parameters related to storm surge overflow and wave overtopping.

A reliable levee slope protection alternative must withstand the applied hydrodynamic forcing. And it is important to remember that a levee designed to resist a given steady overflow discharge magnitude might not be capable of withstanding similar discharge magnitudes resulting from wave-only, or combined wave and surge overtopping. Unsteady overtopping flows have additional effects, including acceleration and deceleration of the flow, and time-varying water depth along the landward-side slope as seen in the photographs of Figure 1. Permissible flow velocity and shear stress are the parameters commonly used to evaluate effectiveness of levee protection systems. This CHETN provides preliminary methods for estimating shear stresses occurring on the landward-side slopes of levees overtopped by a combination of waves and storm surge steady overflow.

Figure 1. Sequence of wave overtopping on a scale-model levee.

SUMMARY OF USACE EXPERIMENTS: Combined storm surge overflow and wave overtopping of a levee with a trapezoidal cross section was studied in a two-dimensional laboratory flow/wave flume at a nominal prototype-to-model length scale of 25-to-1. The experiments were conducted in a 3-ft-wide wave flume at the U.S. Army Engineer Research and Development Center (ERDC), Coastal and Hydraulics Laboratory (CHL) in Vicksburg, MS. The tested levee cross section replicated in the physical model is shown in Figure 2.

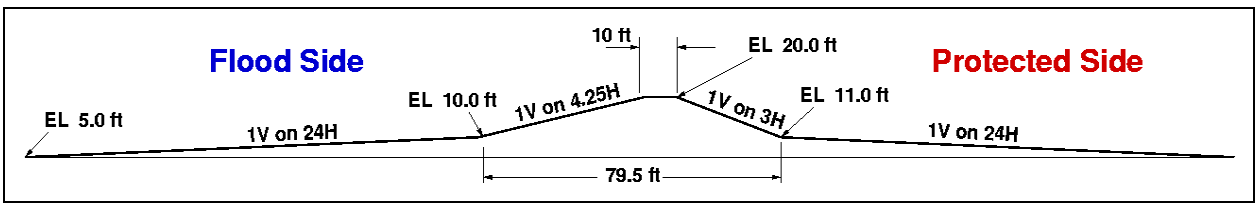

Figure 2. Levee cross section tested in physical model (full-scale dimensions).

This cross section was typical of the Mississippi River Gulf Outlet that experienced severe overtopping during Hurricane Katrina. The model cross section was constructed out of high-density foam using a computer-controlled router. Nominal prototype-scale target surge and wave parameters for testing were: three surge elevations (SL = +1.0, +3.0, and +5.0 ft above levee crest), three significant wave heights (H_{m0} = 3.0, 6.0, and 9.0 ft), and three peak wave periods (T_p = 6, 10, and 14 sec). This gave a total of 27 unique conditions for combined surge and wave overtopping.

Time series of flow depth at two locations on the levee crown and at five locations on the landward-side slope (P1-P7 on Figure 3) were measured using embedded pressure cells. Time series of horizontal flow velocity at the location of P2 near the landward edge of the crown were recorded using a laser Doppler velocimeter. The instantaneous discharge per unit length over the levee crest at each time step was estimated at location P2 as the product of horizontal velocity and water depth. This estimate assumes that velocity is horizontal and constant throughout the water column at this particular location. Incident wave characteristics were measured at a three-gauge array located seaward of the levee. An example of the time-varying flow depth at locations P3 to P7 on the landward-side slope is shown on Figure 4 with the data scaled to prototype dimensions.

Technical Note CHETN-III-78 (Hughes 2008) provides analyses of the measurements and predictive equations for estimating average overtopping discharge, distribution of instantaneous overtopping discharge, and several flow parameters on the landward-side slope such as mean flow thickness,

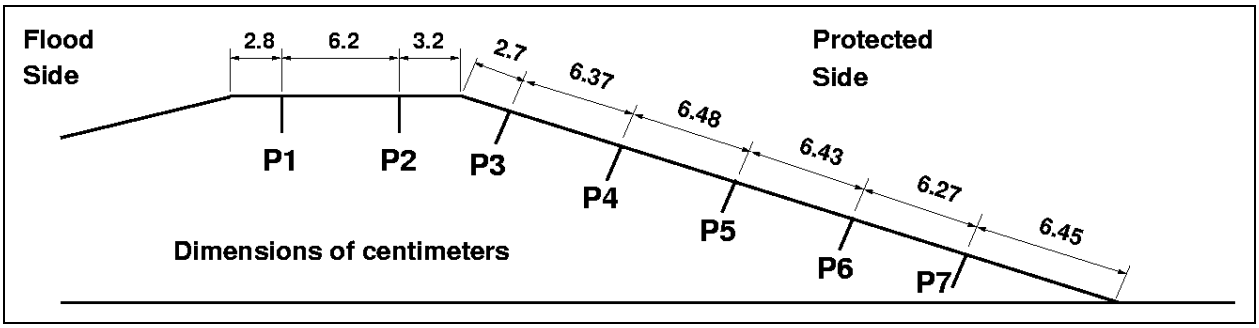

Figure 3. Locations of flush-mounted pressure cells on levee model (model-scale dimensions).

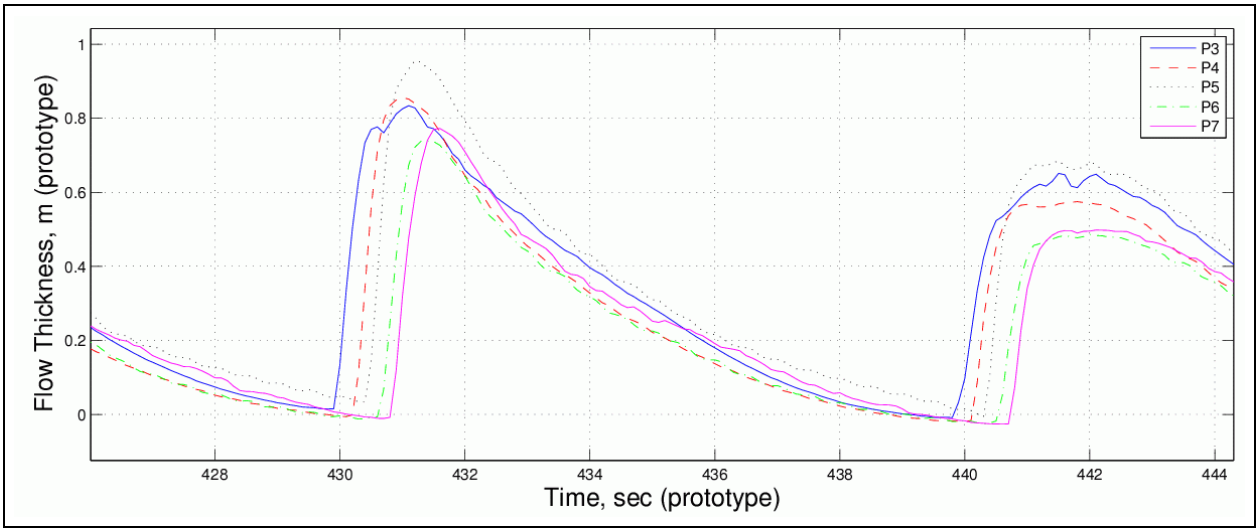

Figure 4. Time-varying flow depth on levee landward-side slope (prototype-scale dimensions).

mean velocity, parameters of the Rayleigh-distributed overtopping wave heights, and the velocity of the wave leading edge. Some of the equations presented in CHETN-III-78 are used in this technical note to estimate shear stresses, and the necessary equations are reproduced here.

SHEAR STRESS DUE TO UNSTEADY, NON-UNIFORM OVERTOPPING FLOW: In the analysis of one-dimensional, unsteady flows, the unknown variables are depth and velocity as functions of both spatial distance and time. The continuity and momentum principles constitute the governing equations required for the solution of these unknown variables. The set of two partial differential equations, corresponding to the continuity and momentum principles, is known as *dynamic wave*, or *Saint-Venant*, equations (Sturm 2001). The Saint-Venant momentum equation for estimating shear stresses on the landward-side slope of earthen levees can be derived by considering the incremental volume of water shown in Figure 5. From Newton's second law the inertial force acting on the incremental volume is balanced by the sum of all external forces. For non-uniform flow on the levee slope, the external forces acting on the incremental volume are due to gravity (weight of water), the change of static pressure, and the frictional resistance of the levee slope surface material.

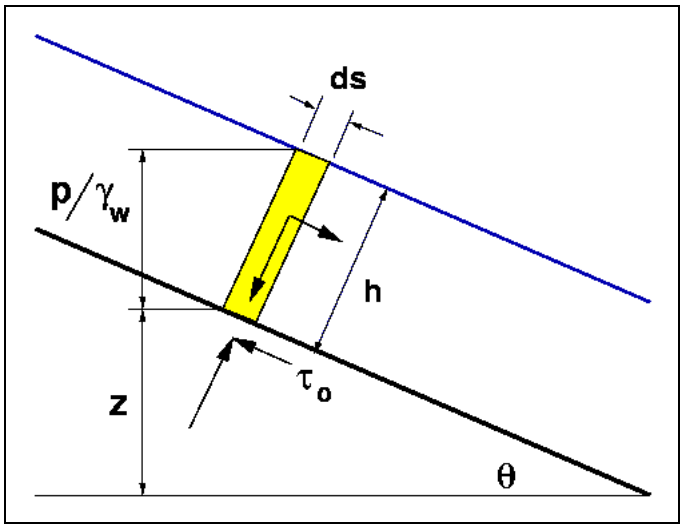

Figure 5. Definition sketch of flow on the landward-side slope of a levee.

The variables shown in Figure 5 are defined as follows:

τ_0 = shear stress
γ_w = specific weight of water
p = hydrostatic pressure
h = flow thickness perpendicular to the slope
θ = angle of levee slope to horizontal
s = down-slope coordinate
z = vertical elevation

Considering only the one-dimensional case of a very wide channel (i.e., long-crested levee) with the major axis aligned with the levee slope, the momentum equation applicable to steep slopes can be written as

$$\frac{\partial v}{\partial t} + v\frac{\partial v}{\partial s} + g\frac{\partial h}{\partial s} + g\,S_f - g\sin\theta = 0 \tag{1}$$

or

$$S_f = \frac{\tau_0}{\gamma_w h} = \sin\theta - \frac{\partial h}{\partial s} - \frac{\partial}{\partial s}\left(\frac{v^2}{2g}\right) - \frac{1}{g}\frac{\partial v}{\partial t} \tag{2}$$

where:

S_f = friction slope
v = flow velocity parallel to the slope
g = acceleration of gravity
t = time

In the derivation of Equation 1 the shear stress was given by the expression

$$\tau_0 = \gamma_w \, h \, S_f \tag{3}$$

with the friction slope, S_f, defined as the net change in energy (head) between two locations along a bottom boundary.

The first term in Equation 1 is the temporal acceleration, the second term is the convective acceleration, the third term represents the change of pressure along the slope, the fourth term comes from the slope resistance friction (Equation 3), and the fifth term is due to the weight of water on the slope. The forms of the momentum equation given by Equations 1 and 2 are valid for unsteady, non-uniform one-dimensional flows, and they are suitable for analyzing unsteady flows due to wave overtopping or combined wave and surge overtopping.

Omitting the fourth term (temporal acceleration) on the right-hand side of Equation 2 yields a somewhat simpler equation valid for steady, non-uniform flow. This form of the momentum equation can be applied on the upper portion of the landward-side slope during steady overflow where the supercritical flow is still accelerating. The steady, uniform flow condition is represented by omitting all but the first term on the right-hand side of Equation 2, which then reduces to a balance between the weight of the water and the frictional resistance given by the familiar steady flow formulation that is a special case of Equation 3, i.e.,

$$\tau_0 = \gamma_w \, h \sin\theta \tag{4}$$

Equation 4 is strictly valid only for steady overflow at a down-slope location where terminal velocity has been reached. For small slope angles, $\sin\theta \approx \tan\theta \approx \theta$ (expressed in radians), but that approximation is not appropriate for structures with steep slopes such as levees. According to Henderson (1966), slopes are regarded as very steep if $\sin\theta$ is greater than 0.01. For comparison purposes, the levee cross section presented in Figure 2 has a value of $\sin\theta$ equal to 0.316.

SHEAR STRESS ANALYSIS: Estimation of shear stress on the landward-side levee slope due to unsteady, non-uniform overtopping flow requires sufficient measurements at a minimum of two locations down the slope sufficient to evaluate a discrete version of Equation 2. Necessary measurements are synoptic time series of slope-perpendicular flow depth and slope-parallel flow velocity at two down-slope locations. The experiment measurements for the tests described earlier included synoptic time series of flow depth, but flow velocity was measured only at one location (above position P2 on Figure 3). In this section several methods are described that were used to approximate the time series of shear stress for each experiment using the measured data.

During the experiments the steady overflow condition was established first, then wave generation was begun. Data collection started at the same instant the wave board was started, so the initial time series (between 700 to 900 data points) captured just the steady overflow. Therefore, the shear stress analyses described below was performed for steady overflow (data points 1–500) and for combined wave and surge overtopping (data points 1,000–15,000).

Shear Stress Estimates Assuming S_f Includes Only the Levee Slope: As a first approximation, the unsteady overtopping flow can be analyzed as steady flow with the momentum equation reduced to the weight of the water associated with the average flow depth balanced by the bottom shear stress. In this case it is assumed that the friction slope is equal to only the levee slope. For an estimate of the mean shear stress by this simple approximation, Equation 2 reduces to

$$\tau_{0,mean} = \gamma_w \, \eta_m \, \sin\theta \tag{5}$$

where η_m is the mean unsteady flow depth perpendicular to the levee slope, and $\tau_{0,mean}$ is the mean shear stress during the overtopping event. Equation 5 can be evaluated using only the mean value of the flow thickness time series measured at any location on the levee landward-side slope. This first approximation for mean shear stress is probably quite reasonable because, on average, the levee slope is several times the magnitude of both the temporal and convective acceleration terms contained in the friction slope, S_f. However, the time series of instantaneous shear stresses estimated by this method using Equation 4 is not expected to be reliable because it lacks the water surface slope and acceleration terms.

Shear Stress Estimates Assuming S_f Includes Levee Slope and Water Surface Slope: The next level beyond the steady flow approximation is to assume the flow does not accelerate or decelerate significantly between two locations (e.g., P1 and P2), so the acceleration terms can be neglected and Equation 2 reduces to the form

$$\tau_0 = \gamma_w \, h_{12} \left[\sin\theta - \frac{\partial h}{\partial s} \right] \tag{6}$$

with the friction slope approximated as a function of the levee slope and the water surface slope. In other words, velocities are not required for this estimate. At each instant in time the slope of the water surface is evaluated using the flow depths at each location, and the flow depth, h_{12}, is the average of the depth at the two locations. Equation 6 can be evaluated using synoptic time series of flow thickness at two locations on the levee landward-side slope to estimate a corresponding time series of shear stress. Each shear stress in the time series represents a spatial mean covering the distance between the two measurement locations at each instant in time. The mean shear stress, $\tau_{0,mean}$, is found as the mean of the generated shear stress time series.

Shear Stress Estimation Assuming Unsteady, Non-Uniform Flow: The most accurate estimate of the shear stress time series is found using the complete version of Equation 2 that is repeated below

$$\tau_0 = \gamma_w \, h_{12} \left[\sin\theta - \frac{\partial h}{\partial s} - \frac{\partial}{\partial s}\left(\frac{v^2}{2g} \right) - \frac{1}{g}\frac{\partial v}{\partial t} \right] \tag{7}$$

Estimating the time series of shear stress using Equation 7 is difficult for these experiments because no direct measurements of flow velocity were acquired on the landward-side slope coincident with flow depth measurements. However, an estimate of the instantaneous discharge time series for each

of the 27 experiments was made by multiplying coincident values of flow depth, h, and flow velocity, v, at location P2 shown on Figure 3. Hughes (2008) observed the close similarity in flow depth time series between gauges P4 and P7, and he was able to shift the P4 time series in time to overlay the P7 time series. The overlain time series matched closely with differences in peak magnitudes attributed to flow acceleration between the two locations, implying that the individual waves were moving down the slope with only minor transformation. In other words, the waves had nearly permanent form over the short down-slope distance.

The flow depth time series from location P2 were shifted in time to overlay with time series from locations P4 and P7. Good correspondence was seen in the locations of wave crests and troughs, and the general form of the time series was maintained, but the flow depth magnitudes were quite different (less) because of velocity magnitude differences. Based on the correspondence between the P2 time series and time series recorded on the levee landward-side slope, the extremely tentative assumption was made that the overtopping instantaneous discharge time series does not change significantly over the short distances from the levee crest to the toe of the landward-side slope. Therefore, it would be reasonable as a first estimate to time-shift the measured discharge time series down the slope until the peak discharges aligned with the maximum flow depths at the leading edge of the wave at the locations P4 and P7. Then, the synthetic velocity time series at locations P4 and P7 were estimated by dividing the time-shifted discharge time series by the flow depth time series at P4 and P7, i.e., $v(t) = q(t)/h(t)$; where $q(t)$ is the discharge time series per unit crest length.

Care was taken during the velocity time series estimation procedure to avoid generating unrealistic peak velocities. Because the front of each wave is very steep, occasionally the maximum discharge for a wave would be matched with a flow depth less than the maximum of the wave front, and this gave a velocity that was too large. To mitigate this problem, the maximum velocity at the wave front was constrained to the value estimated by dividing the maximum discharge of the wave by the maximum flow depth.

Using this methodology, estimates of the velocity time series were constructed at locations P4 and P7 for all 27 experiments. These synthetic velocity time series were used in conjunction with the coincident measured flow depths to develop corresponding time series of shear stress using Equation 7. At each time step, the flow depth h_{12} was taken as the average of the depths measured at P4 and P7. The convective acceleration term was estimated as the velocity difference (Δv) between locations P4 and P7 at that time step divided by the down-slope distance (Δs). The temporal acceleration term was estimated as the velocity difference at each instant in time between locations P4 and P7 (Δv) divided by the time shift (Δt) required to align the wave peaks from the flow depth time series measured at locations P4 and P7. Each shear stress value in the time series represents a spatial mean covering the distance between the two measurement locations at each instant in time. The mean shear stress, $\tau_{0,mean}$, was found as the mean of the generated shear stress time series.

SHEAR STRESS RESULTS: Equations 5, 6, and 7 were used to estimate shear stresses for all 27 experiments. The specific weight of water was taken as fresh water with γ_w = 62.4 lb/ft^2. Equation 5 assumes the friction slope is equal to the levee slope; and the mean shear stress, $\tau_{0,mean}$, was calculated as the average of the mean shear stress estimated at P4 and at P7 using only the mean

of the measured flow depths. Thus, the mean shear stress represents the average shear stress acting on the levee slope between these two locations, a distance of 15.7 ft at prototype scale.

Equation 6 assumes the friction slope is equal to the combined levee slope and slope of the water surface. The resulting shear stress time series represents the time-varying average shear stress acting over the distance between locations P4 and P7. The mean shear stress is the mean of the calculated shear stress time series.

Equation 7 uses the complete definition of friction slope, and it would be the most accurate provided the synthesized velocity time series are reasonably correct. The calculated shear stress time series represent the spatial average over the distance between locations P4 and P7.

As mentioned, the first 500 measurement points represent only the steady overflow in the experiment, whereas data points 1,000 to 15,000 measured combined wave and surge overtopping. The mean shear stress was estimated using the three methods for both the steady overflow and the combined wave and surge overtopping portions for all experiments. It is important to remember that the shear stress estimates given in the following section are strictly applicable only for levees having slope surface roughness similar to the smooth slopes used in the physical model. In other words, the roughness in the physical model probably is closer to representing smooth, grass-covered levees than levees armored with stone riprap.

Steady Overflow Shear Stress Results: Table 1 presents the values for average shear stress calculated for the steady overflow portion of the experiments using the three methods described above. The first column is the experiment identifier, and column 2 is the measured steady overflow discharge scaled to prototype scale using a prototype-to-model scale ratio of 25-to-1. Columns 3–5 compare the estimated mean shear stresses.

There is not much difference between the estimates when the surge level was only 0.95 ft above the levee crest (freeboard R_c = -0.95 ft), and this indicates that approximating the friction slope as the levee slope is reasonable for estimating mean shear stress resulting from small values of negative freeboard. However, as surge level increased the mean shear stress estimates that included the acceleration terms were smaller than estimates using Equations 5 and 6. This indicates the actual friction slope is less than the levee slope because the flow is still accelerating down the levee landward-side slope. In other words, the levee slope needed to be longer in order for the flow to reach terminal velocity.

Combined Wave and Surge Overtopping Shear Stress Results: Shear stress estimates for the unsteady flow created by combined surge overflow and wave overtopping are shown in Table 2. Columns 2 and 3 give the incident wave conditions scaled to prototype values, and column 4 is the average combined wave and surge overtopping discharge, q_{ws}, estimated from the discharge time series. Values of mean shear stress estimated by the three methods described above are given in columns 5–7.

Table 1
Mean Shear Stress Estimates for Steady Surge Overflow

Exp. No.	Prototype-Scale q_s (ft^2/sec)	$\tau_{0,mean}$ (lb/ft^2) Equation 5	Equation 6	Equation 7
Surge Level = +0.95 ft Above Levee Crown				
R128	2.86	3.8	3.8	4.0
R129	3.32	3.5	3.5	4.4
R130	3.09	3.2	3.2	4.1
R104	2.79	4.9	4.9	5.1
R105	2.60	4.5	4.5	4.5
R131	2.59	3.8	3.8	3.9
R107	2.66	3.7	3.7	3.1
R108	2.78	5.6	5.7	4.8
R109	2.81	4.7	4.8	4.4
Surge Level = +2.66 ft Above Levee Crown				
R110	12.43	15.7	15.8	14.4
R111	13.06	16.0	16.1	15.2
R112	12.71	16.2	16.6	13.6
R113	12.11	16.0	16.3	14.2
R132	17.23	16.3	16.4	14.2
R115	13.44	17.2	17.5	15.1
R116	12.62	16.5	16.8	14.6
R117	13.45	17.3	17.6	15.9
R118	13.32	17.4	17.7	15.8
Surge Level = +4.27 ft Above Levee Crown				
R119	26.41	30.0	31.8	22.2
R120	27.18	29.4	31.0	21.1
R121	27.41	29.7	31.4	21.1
R122	28.30	30.2	31.8	21.9
R123	27.23	29.8	31.2	23.1
R124	27.85	30.6	32.5	21.1
R125	26.01	29.8	31.1	23.7
R126	26.64	29.8	31.6	22.0
R127	27.31	31.6	33.3	24.2

Just as in the steady overflow case, mean shear stress estimates calculated using accelerations in the friction slope (column 7) are similar to the other estimates for R_c = -0.95 ft. But as the surge overflow level increased, the shear stresses estimated using the complete description of friction slope become progressively less than estimates made using only the levee slope or a combination of the levee and water surface slope.

Table 2
Mean Shear Stress Estimated for Unsteady Combined Wave and Surge Overtopping

Exp. No.	Prototype-Scale			$\tau_{0,mean}$ (lb/ft^2)		
	H_{m0} (ft)	T_p (sec)	q_{ws} (ft^2/sec)	Equation 5	Equation 6	Equation 7
Surge Level = +0.95 ft Above Levee Crown						
R128	2.69	6.07	4.07	6.4	6.4	7.1
R129	5.47	5.94	5.30	9.3	9.2	10.5
R130	8.33	5.94	5.60	11.7	11.7	13.1
R104	3.29	10.51	3.20	7.4	7.4	7.4
R105	6.20	10.51	5.30	11.0	11.1	10.9
R131	9.27	10.51	7.84	14.6	14.7	15.0
R107	2.58	13.66	3.78	7.5	7.5	7.1
R108	5.52	13.66	5.93	11.8	12.0	11.6
R109	8.15	13.66	7.49	15.6	15.7	15.6
Surge Level = +2.66 ft Above Levee Crown						
R110	2.53	5.69	12.71	17.3	17.6	15.7
R111	4.80	5.94	11.82	18.3	18.6	17.7
R112	7.89	5.94	11.42	20.5	21.2	19.9
R113	2.88	10.12	11.78	17.2	17.6	15.6
R132	6.27	10.12	17.44	19.3	19.8	16.9
R115	8.74	10.51	15.41	22.7	23.0	22.1
R116	2.46	14.37	13.45	18.2	18.6	16.2
R117	5.36	11.38	15.61	20.8	21.4	18.9
R118	7.92	14.37	16.23	23.9	24.1	23.2
Surge Level = +4.27 ft Above Levee Crown						
R119	2.10	6.07	27.73	33.0	35.0	24.0
R120	3.84	6.07	28.60	33.5	35.3	25.4
R121	7.55	6.07	28.74	34.5	35.9	29.7
R122	2.83	10.12	28.21	32.8	34.5	24.9
R123	5.86	10.12	29.82	34.3	35.7	28.8
R124	8.99	10.12	29.69	35.8	36.8	33.0
R125	2.43	14.37	27.82	32.5	33.8	26.4
R126	4.92	14.37	29.43	34.7	36.5	27.7
R127	7.59	14.37	30.56	37.6	37.9	35.7

Figure 6 compares the mean shear stress values based only on the bottom slope, S_0 (Equation 5) to mean shear stresses estimated using the friction slope, S_f (Equation 7). The solid line is the line of equivalence. At the lowest negative freeboard, R_c = -0.95 ft, mean shear stress estimates based on only the bottom slope, S_0, are essentially the same as estimates based on the friction slope.

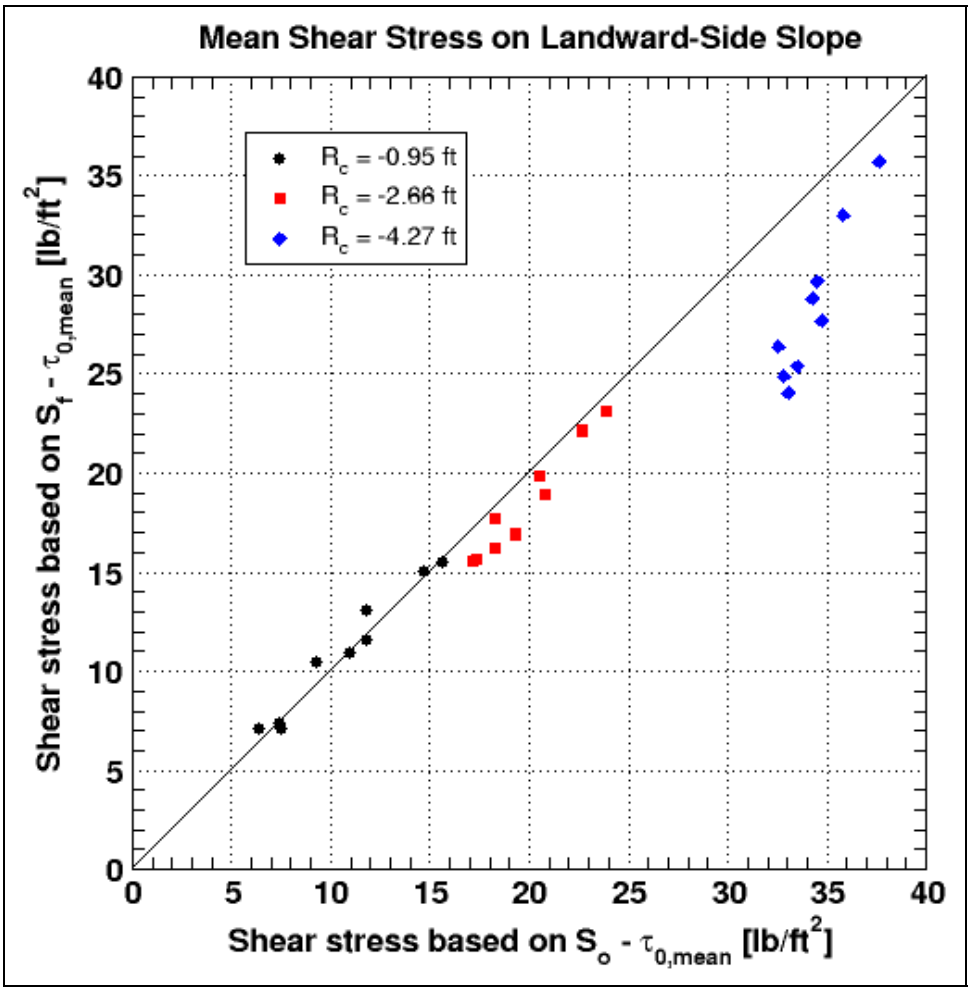

Figure 6. Comparison of mean shear stress calculated from bottom slope and friction slope.

This implies that mean shear stress can be estimated for low negative freeboards using only the mean flow thickness on the landward-side slope. For R_c = -2.66 ft, the comparisons are still similar, but the mean shear stress values estimated using S_0 have a tendency to over-predict slightly the mean shear stress calculated based on the friction slope, S_f. For R_c = -4.27 ft, however, mean shear stresses estimated using S_0 over-predict the mean shear stress based on friction slope by as much as 38 percent. Thus, at larger negative freeboards, the friction slope is significantly less than the levee slope because the flow is still accelerating and has not yet approached terminal velocity.

Using both the bottom slope and the water surface slope, *dh*/*ds*, to estimate mean shear stress (Equation 6) did not improve the comparison, indicating there is no clear benefit gained by including water surface slope but neglecting accelerations in the calculation. Actually, first-order estimates obtained by assuming friction slope equals levee slope (Equation 5) resulted in better predictions than using the more complex Equation 6.

PREDICTION OF MEAN SHEAR STRESSES: An empirical relationship was sought between the hydrodynamic parameters for each experiment and the corresponding mean shear stress estimated using Equation 7. The best correspondence was found as a best-fit of the data to be a simple expression relating the mean shear stress to the specific weight of fresh water, γ_w, and the root-mean-square of the flow depth perpendicular to the levee slope, η_{rms}, i.e.,

$$\tau_{0,mean} = 0.235\, \gamma_w\, \eta_{rms} \tag{8}$$

Figure 7 shows a plot of the mean shear stress correlation with Equation 8 drawn as the solid line. The correlation coefficient for this best-fit equation was 0.992 with an RMS percent error of 0.071. Equation 8 is similar in form to the basic shear stress definition given by Equation 3. It is important to reiterate that Equation 8 applies only to smooth slopes having similar frictional resistance as the levee model used in the tests.

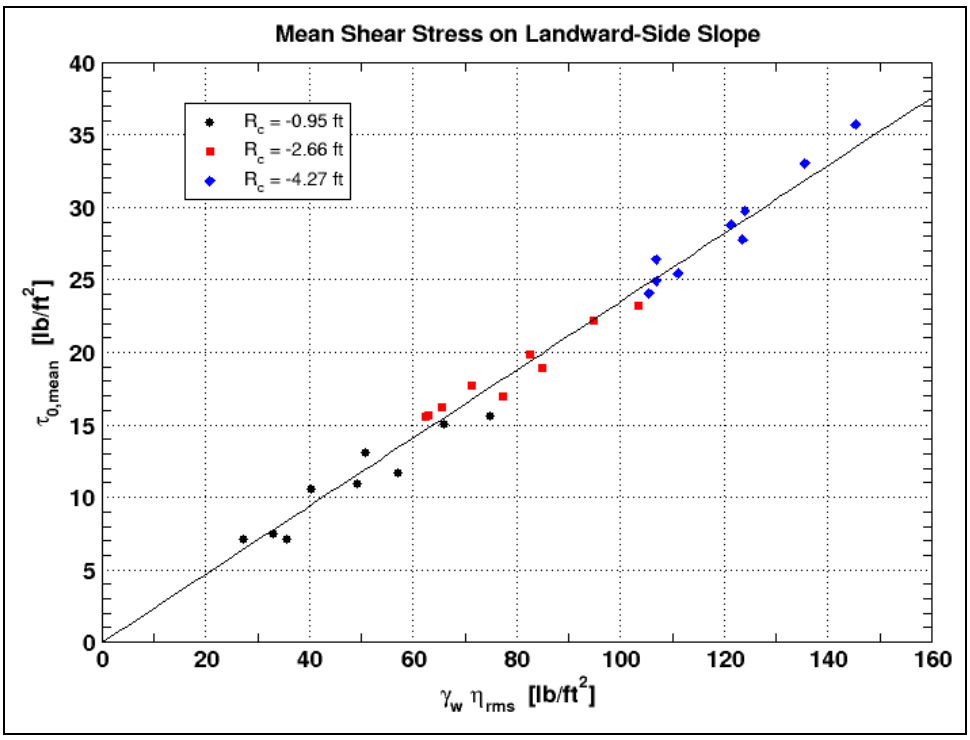

Figure 7. Mean shear stress as a function of η_{rms}.

Estimation of mean shear stress using Equation 8 requires an expression for the root-mean-squared flow thickness, η_{rms}, in terms of the forcing hydrodynamic parameters. A reasonable empirical correlation is given by the following expression

$$\frac{\eta_{rms}}{\eta_m} = 1 + 0.0077 \left(\frac{g\, H_{m0}\, T_p}{q_{ws}} \right)^{2/3} \tag{9}$$

where η_m is the mean flow thickness, H_{m0} is the incident energy-based significant wave height, T_p is the spectrum peak wave period, and q_{ws} is average combined wave and surge overtopping discharge per unit crest length. Figure 8 plots the measurements for all 27 experiments. The solid line is Equation 9 which had a correlation coefficient of 0.952 and an RMS percent error of 0.032.

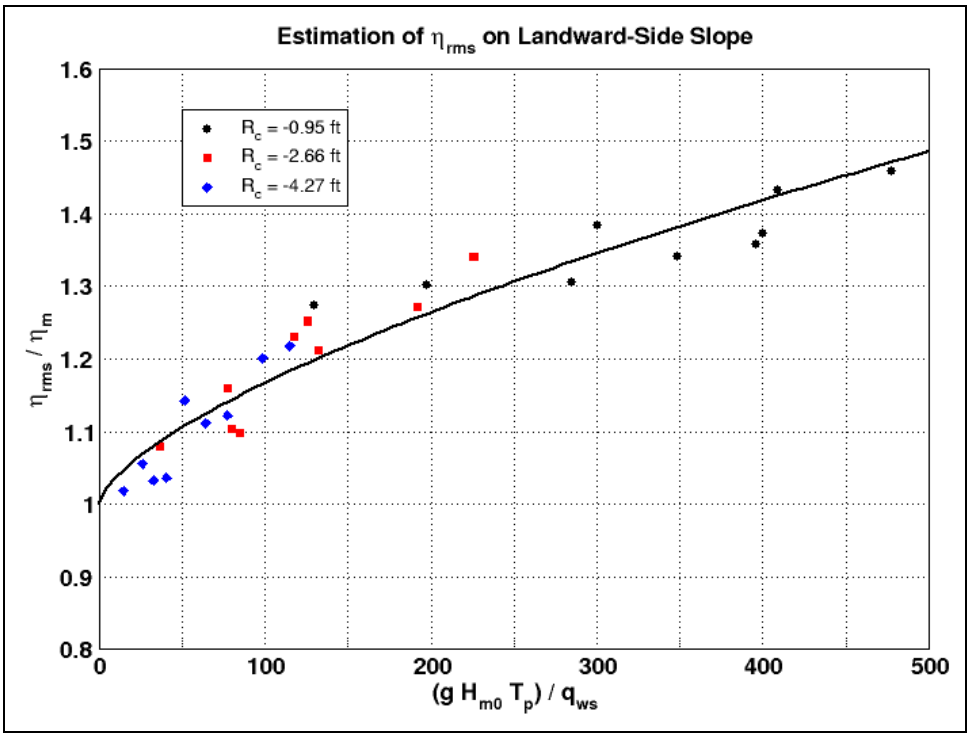

Figure 8. Empirical relationship for the ratio η_{rms} / η_m.

Hughes (2008) provided the following empirical equations to estimate values of η_m and q_{ws} associated with combined wave and surge overtopping that are needed in Equation (9).

$$\eta_m = 0.4 \left[\frac{1}{g \sin\theta} \right]^{1/3} (q_{ws})^{2/3} \tag{10}$$

and

$$\frac{q_{ws}}{\sqrt{g\ H_{m0}^3}} = 0.0336 + 0.53 \left(\frac{-R_c}{H_{m0}} \right)^{1.58} \tag{11}$$

where:

θ	=	angle of the landward-side levee slope with the horizontal
q_{ws}	=	average discharge due to combined waves and surge per unit crest length
H_{m0}	=	energy-based significant wave height
R_c	=	freeboard (negative when surge elevation exceeds levee crest elevation)
g	=	acceleration of gravity

Because each of the empirical equations used to estimate the mean shear stress involves some scatter in the measurements, an overall evaluation of the estimation procedure skill is seen by comparing the mean shear stress based on measurements to estimates obtained using Equations 8–11. This comparison is shown in Figure 9. Overall, the equations provide reasonable estimates indicating there is not distinct bias in the correlations. Remember that these estimates are applicable only to smooth levee slopes.

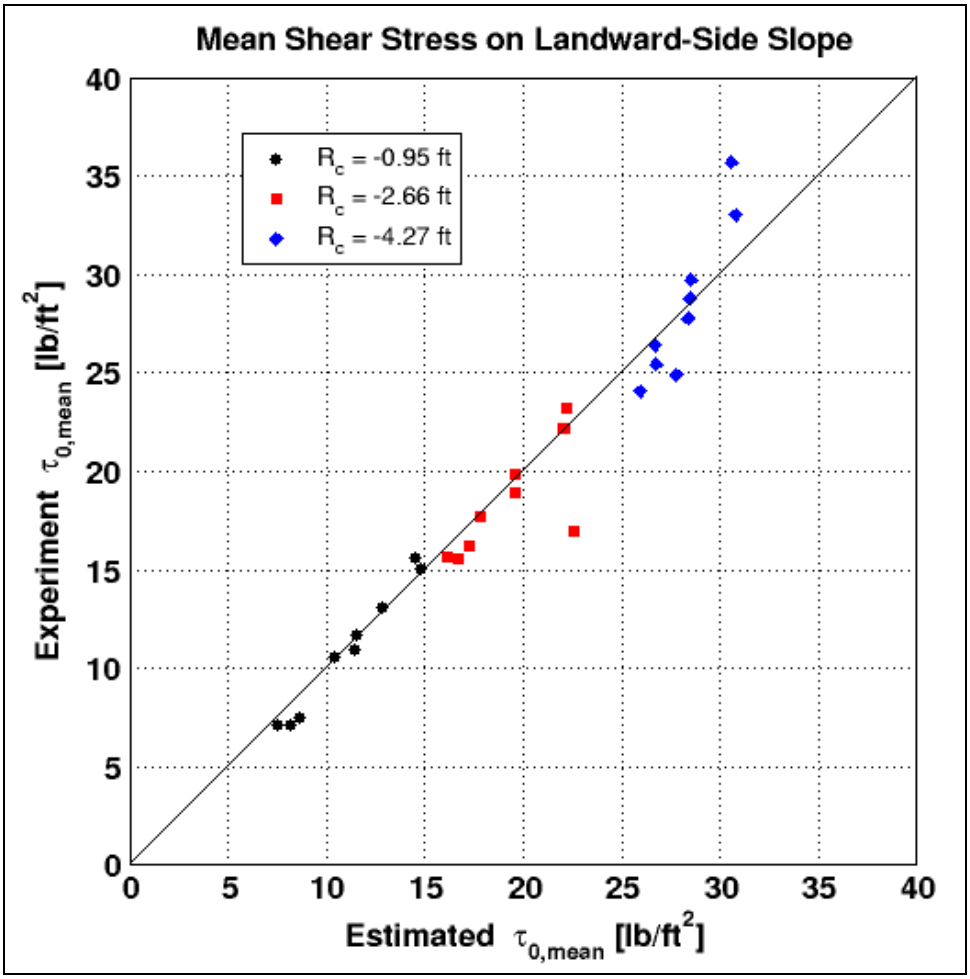

Figure 9. Calculated versus experiment mean shear stress.

ESTIMATION OF EXTREME SHEAR STRESS VALUES: The mean shear stress values estimated by the method given above provide an overall average that occurs during a combined wave and surge overtopping event. However, in the time series of instantaneous shear stress acting on the landward-side slope, the peak stresses associated with the overtopping wave crests can be several times the magnitude of the mean shear stress. The peak shear stress acts for a short duration as the wave passes down the slope, but the peak shear stress may well be the defining parameter with respect to stability of armoring alternatives or for determining rates of soil erosion.

The calculated time series of instantaneous shear stress were analyzed in the time domain using standard up-crossing analysis. The maximum shear stress values for each identified wave were rank-

ordered, and representative values were determined for the average of the highest 1/3, highest 1/10, and highest 1/100 of the peak shear stresses. These values were denoted as $\tau_{0,1/3}$, $\tau_{0,1/10}$, and $\tau_{0,1/100}$, respectively. Similar to the case of mean shear stress (Equation 8), good correlations were found between the representative peak shear stresses and the product of specific weight of water, γ_w, and a representative measure of flow depth given by the root-mean-square wave height on the landward-side levee slope, H_{rms}. The resulting correlations are shown on Figure 10. Notice the high magnitudes of peak shear stress on Figure 10 compared to the mean values given on Figure 7.

The solid lines on Figure 10 are the best-fit linear equations given as

$$\tau_{0,1/3} = 0.53\,\gamma_w\,H_{rms} \tag{12}$$

$$\tau_{0,1/10} = 0.69\,\gamma_w\,H_{rms} \tag{13}$$

$$\tau_{0,1/100} = 0.93\,\gamma_w\,H_{rms} \tag{14}$$

Correlation coefficients for Equations 12, 13, and 14 were 0.973, 0.968, and 0.941, respectively. The corresponding RMS percent errors were 0.154, 0.199, and 0.277. As seen in Figure 10 the correlations are reasonable with greater scatter shown for the more extreme shear stresses.

Application of Equations 12–14 requires an estimate of H_{rms} perpendicular to the landward-side slope. Hughes (2008) provided the following empirical equation for estimating H_{rms} as a function of freeboard (R_c), incident significant wave height (H_{m0}), and mean flow thickness (η_m).

$$\frac{H_{rms}}{\eta_m} = 3.43 \cdot \exp\left(\frac{R_c}{H_{m0}}\right) \tag{15}$$

Freeboard must be entered as a negative number for the case of combined wave and surge overtopping, and the appropriate value for η_m is determined using Equation 10. Based on the relatively good fit of the data shown in Figure 10, it was concluded that Equations 12–15 provide a reasonable estimate for the more extreme shear stresses that can occur on levee slopes having a relatively smooth surface.

PERMISSIBLE SHEAR STRESS VALUES: Permissible shear stress criteria associated with the different levee slope protection and armoring alternatives are not commonly found in the literature. However, there are numerous estimates of permissible shear stress for soils and stone linings. Some of these estimates are presented in this section in order to put in perspective the magnitude of the shear stress values associated with combined wave and storm surge overtopping as estimated in this CHETN.

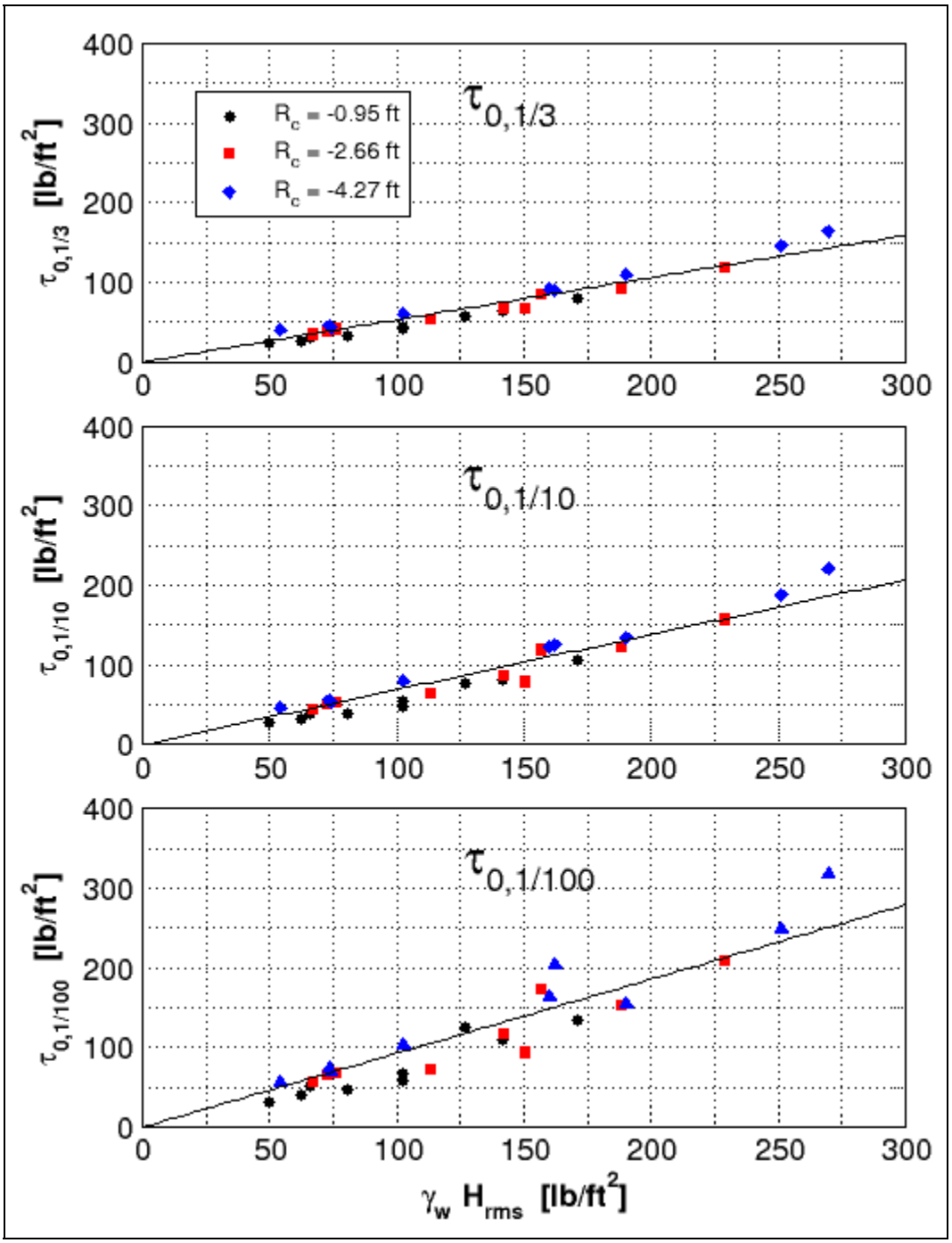

Figure 10. Representative peak shear stress parameters.

The Federal Highway Administration's HEC-15 publication (FHWA 2005) provides typical values of permissible shear stress for selected lining types. Table 3 extracts some of the examples presented in HEC-15. Note that these shear stress values were estimated based on different equations then presented in this CHETN.

Table 3
Permissible Shear Stress for Bare Soils and Stone Linings (after FHWA 2005)

Lining Category	Lining Type	Permissible Shear Stress (lb/ft^2)
Cohesive bare soil	Clayey sands	0.037 – 0.095
	Inorganic silts	0.027 – 0.11
	Silty sands	0.024 – 0.072
	Inorganic clays	0.14
Non-cohesive bare soil	Finer than coarse sand, d_{75} < 0.05	0.02
	Fine gravel, d_{75} < 0.3 in	0.12
	Gravel, d_{75} < 0.6 in	0.24
Gravel mulch	Coarse gravel d_{50} < 1 in	0.4
	Very coarse gravel d_{50} < 2 in	0.8
Rock riprap	0.5 ft < d_{50} < 1.0 ft	2.4 – 4.8

Fortier and Scobey (1926) published a table of permissible channel velocities for well-seasoned channels of small slopes and flow depths less than 3 ft. These values of permissible velocities are shown in Table 4 along with associated permissible shear stresses as described and tabulated in Chow (1959). The values of permissible shear stress given in Chow (1959) more or less agree with those shown in Table 3.

Also shown in the rightmost column of Table 4 are values of permissible shear stress presented by the Independent Levee Investigation Team (ILIT) (2006) that conducted an investigation of the failure of New Orleans' levees during Hurricane Katrina. Using the same permissible velocities given by Fortier and Scobey (1926) and shown in Table 4, the ILIT estimated permissible shear stress using the equation given in Munson et al. (1990) for turbulent pipe flow, i.e.,

$$\tau_o = K \rho_w \frac{v^2}{2} \tag{16}$$

where K is a constant dependent on the surface roughness of the pipe, and ρ_w is water density. Munson et al. (1990) showed that Equation 16 can be expressed as the Chezy equation with the Chezy coefficient equal to

$$C_Z = \sqrt{\frac{2g}{K}} \tag{17}$$

Therefore, the surface roughness constant, K, is nothing more than the Fanning friction factor, f_F (Hughes 2007). The values of permissible shear stress calculated by the ILIT assumed $K = 1$, which is too large by a factor of 50 to 100. A more appropriate value would have been $K = f_F = 0.015$. This explains why the values of permissible shear stress presented by the ILIT do not agree with previous established values. A method for approximating f_F in terms of flow depth and Mannings n is given in Hughes (2007).

Table 4
Permissible Shear Stress for Average Flow Depth of 3 Ft (Chow 1959; ILIT 2006)

Material	Velocity Range (ft/sec)	Permissible Shear Stress (lb/ft^2)	
		Chow (1959)	ILIT (2006)
Fine sand (colloidal)	1.5 – 2.5	0.027 – 0.075	2.4 – 6.3
Sandy loam (noncolloidal)	1.75 – 2.50	0.037 – 0.075	3.1 – 6.3
Silt loam (noncolloidal)	2.00 – 3.00	0.048 – 0.11	4.0 – 9.0
Alluvial silt (noncolloidal)	2.00 – 3.50	0.048 – 0.15	4.0 – 12.3
Ordinary firm loam	2.50 – 3.50	0.075 – 0.15	6.3 – 12.3
Fine gravel	2.50 – 5.00	0.075 – 0.32	6.3 – 25.0
Stiff clay	3.75 – 5.00	0.26 – 0.46	14.1 – 25.0
Alluvial silt (colloidal)	3.75 – 5.00	0.26 – 0.46	14.1 – 25.0
Coarse gravel (noncolloidal)	4.00 – 6.00	0.30 – 0.67	16.0 – 36.0
Shales and hardpans	6.0	0.67	36.0

Note that the permissible shear stresses shown in Tables 3 and 4 are for subcritical flow in mild sloped channels, and they may not appropriate for high-velocity supercritical flows occurring on the steep landward-side slopes of overtopped levees. Furthermore, it is well established that healthy vegetation on levee slopes increases the erosion resistance of soils by a large amount. For example, Hanson and Temple (2002) conducted field tests on steep vegetated and non-vegetated channels subjected to long-duration supercritical flow. The maximum average erosion rate in the non-vegetated channel was 25 to 50 times greater than that of the vegetated channel even though the soil had a measured critical shear stress of 0.55 Pa (0.01 lb/ft^2). Clearly there is a need to develop allowable shear stress values for a range of levee slope materials and slope protection alternatives.

Example: Shear Stress due to Combined Overtopping

Find: The mean shear stress, as well as the representative peak shear stresses associated with the highest 1/3, 1/10. and 1/100 of the instantaneous shear stress peaks, for wave overtopping combined with overflow by a surge elevation that is 1.3 ft above the levee crest elevation. The levee surface is considered smooth with roughness comparable to grass or turf reinforcement mats.

Given:

H_{m0} = 8 ft = zeroth-moment significant wave height
T_p = 10 sec = wave period associated with the spectral peak
h_c = 15.0 ft = levee crest elevation
h_S = 18.3 ft = storm surge elevation
R_c = -3.3 ft = freeboard [= h_c - h_S]
$\tan \alpha$ = 1/4 = seaward-side levee slope
$\tan \theta$ = 1/3 = landward-side levee slope [θ = 18.4^o]
γ_w = 64.0 lb/ft^3 = specific weight of sea water
g = 32.2 ft/sec^2 = acceleration due to gravity

Although the seaward-side levee slope is not used in these calculations, it is wise to make sure the slope is not too different than the 1-on-4.25 seaward-side slope used in the physical model study on which these equations are based.

Calculate Average Overtopping Discharge. The combined wave/surge overtopping discharge per unit crest length is found using Equation 11

$$\frac{q_{ws}}{\sqrt{g\ H_{m0}^3}} = 0.0336 + 0.53\left(\frac{-R_c}{H_{m0}}\right)^{1.58}$$

$$= 0.0336 + 0.53\left(\frac{-(-3.3\,\text{ft})}{8\,\text{ft}}\right)^{1.58}$$

$$\frac{q_{ws}}{\sqrt{g\ H_{m0}^3}} = 0.164$$

Solving for q_{ws} yields

$$q_{ws} = \sqrt{g\ H_{m0}^3} \times 0.164 = \sqrt{(32.2\,\text{ft/sec}^2)(8\,\text{ft})^3} \times 0.164$$

$$q_{ws} = 21.1\ \text{ft}^2/\text{sec}$$

(Note the discharge units ft^2/sec are equivalent to ft^3/sec per ft or cfs/ft.)

Calculate Flow Parameters on the Landward-Side Levee Slope. Under the assumption that the levee surface roughness is small (similar to the smooth slope used in the laboratory tests), the mean flow thickness perpendicular to the landward-side slope is estimated from Equation 10 as

$$\eta_m = 0.4\left[\frac{1}{g\sin\theta}\right]^{1/3}(q_{ws})^{2/3}$$

$$= 0.4\left[\frac{1}{(32.2\,\text{ft/sec}^2)\sin(18.4^o)}\right]^{1/3}\left(21.1\ \text{ft}^2/\text{sec}\right)^{2/3}$$

$$\eta_m = 0.4\left(0.46\ \text{sec}^{2/3}/\text{ft}^{1/3}\right)\left(7.64\,\text{ft}^{4/3}/\text{sec}^{2/3}\right) = 1.4\ \text{ft}$$

The root-mean-squared flow depth on the landward-side slope can be estimated using Equation 9

$$\eta_{rms} = \eta_m + 0.0077\left(\frac{g\,H_{m0}\,T_p}{q_{ws}}\right)^{2/3} \times \eta_m$$

$$= 1.4\text{ ft} + 0.0077\left(\frac{32.2\,\text{ft/sec}^2 \cdot (8\,\text{ft}) \cdot 10\text{ sec}}{21.1\,\text{ft}^2/\text{sec}}\right)^{2/3} \times 1.4\text{ ft}$$

$$\eta_{rms} = 1.7\text{ ft}$$

The root-mean-squared wave height (perpendicular to the levee slope) is estimated from Equation 15 as

$$H_{rms} = \eta_m\left[3.43 \cdot \exp\left(\frac{R_c}{H_{m0}}\right)\right] = (1.4\,\text{ft})\left[3.43 \cdot \exp\left(\frac{-3.3\,\text{ft}}{8\,\text{ft}}\right)\right]$$

$$H_{rms} = 3.2\text{ ft}$$

Calculate Average Shear Stress on the Landward-Side Levee Slope. The mean shear stress, as a function of the root-mean-squared flow depth, can be estimated from Equation 8

$$\tau_{0,mean} = 0.235\,\gamma_w\,\eta_{rms} = 0.235 \cdot \left(64.0\text{ lb/ft}^3\right) \cdot 1.7\,\text{ft}$$

$$\tau_{0,mean} = 25.6\text{ lb/ft}^2$$

Calculate Peak Shear Stress Parameters on the Landward-Side Levee Slope. The peak shear stress parameters are given as functions of the root-mean-squared wave height.

The peak shear stress corresponding to the average of the highest 1/3 shear stress peaks is estimated from Equation 12

$$\tau_{0,1/3} = 0.53\,\gamma_w\,H_{rms} = 0.53 \cdot \left(64.0\text{ lb/ft}^3\right) \cdot 3.2\,\text{ft}$$

$$\tau_{0,1/3} = 108.5\text{ lb/ft}^2$$

Similarly, the peak shear stress corresponding to the average of the highest 1/10 shear stress peaks is estimated from Equation 13

$$\tau_{0,1/10} = 0.69\,\gamma_w\,H_{rms} = 0.69 \cdot \left(64.0\text{ lb/ft}^3\right) \cdot 3.2\,\text{ft}$$

$$\tau_{0,1/10} = 141.3\text{ lb/ft}^2$$

Finally, the peak shear stress corresponding to the average of the highest 1/100 shear stress peaks is estimated from Equation 14

$$\tau_{0,1/100} = 0.93\,\gamma_w\,H_{rms} = 0.93 \cdot \left(64.0\text{ lb/ft}^3\right) \cdot 3.2\,\text{ft}$$

$$\tau_{0,1/100} = 190.5\text{ lb/ft}^2$$

Note that the peak shear stress parameters estimated for the average of the highest 1/3, 1/10, and 1/100 of the shear stress peaks represent 4.2, 5.5, and 7.4 times the estimated mean shear stress value.

Remarks. This example and the equations used to make shear stress estimates were based on small-scale laboratory experiments with a levee having a smooth slope. The estimated Manning's coefficient for this slope surface varied between n = 0.012 and 0.04 depending on flow thickness. These values were similar to values given in the literature for grass-covered steep slopes. Therefore, the example results would be applicable to grass-covered levees. Application of the equations to levees having significantly rougher slope surfaces (e.g., riprap) would be less reliable and ill-advised.

SUMMARY: This CHETN has summarized new empirical equations for estimating various shear stress parameters for the landward-side slopes of earthen levees being overtopped by a combination of steady overflow due to storm surge and unsteady flow due to wave overtopping. Equations are given for the mean shear stress and for estimating representative shear stress values associated with the average of the highest 1/3, highest 1/10, and highest 1/100 of the shear stress peaks for all the waves.

The empirical equations are based on small-scale laboratory experiments featuring a levee with a seaward-side slope of 1:4.25, and the equations may not be applicable for levees having different seaward-side slopes. It is hypothesized that seaward-side slope may not be as important for combined wave and surge overtopping as it is for wave-only overtopping. A major component in this development was the assumption that the time series of instantaneous overtopping discharge retains its form over the short distance down the landward-side slope. This allowed estimation of the velocity time series using measured time series of flow thickness.

Recommended equations for estimating the landward-side slope mean and RMS flow depths include slope angle and a constant that is likely a function of some representative friction factor characterizing slope roughness. Applicability of these equations for landward-side slopes different than 1-on-3 is uncertain, and the equations will give incorrect estimates where slope surface roughness is not relatively smooth. Finally, the flows down the landward-side slope in the small-scale experiments had little, if any, air entrainment. This is certainly not the case for similar flows at full scale. How this aeration scale effect alters the parameters estimated by the empirical equations is not yet known.

Until additional experiments are conducted to confirm these relationships, the guidance given in this CHETN should be considered as tentative. The next phase of design guidance development is to relate the unsteady shear stress parameters to soil erosion rates and stability of slope protection alternatives.

ADDITIONAL INFORMATION: This CHETN is a product of the Affordable Levee Strengthening and New Design Work Unit being conducted at the U.S. Army Engineer Research and Development Center, Coastal and Hydraulics Laboratory and sponsored by the Department of Homeland Security Levee Strengthening and Damage Mitigation Program. Questions about this technical note can be addressed to Mr. Noberto Nadal, Noberto.C.Nadal@usace.army.mil Beneficial review was provided by Dr. Greg Hanson, Agricultural Research Station, U.S. Department of Agriculture. This document should be cited as follows:

> Nadal, N. C., and S. A. Hughes. 2009. *Shear stress estimates for combined wave and surge overtopping at earthen levees*. Coastal and Hydraulics Engineering Technical Note ERDC/CHL CHETN-III-79. Vicksburg, MS: U.S. Army Engineer Research and Development Center. *http://chl.erdc.usace.army.mil/chetn*.

REFERENCES

Chow, V. T. 1959. *Open-channel hydraulics*. New York: McGraw-Hill.

Federal Highway Administration (FHWA). 2005. *Design of roadside channels with flexible linings*. Hydraulic Engineering Circular No. 15, 3rd Ed. Publication No. FHWA-NHI-05-114.

Fortier, S., and F. C. Scobey. 1926. Permissible canal velocities. *Transactions*, American Society of Civil Engineers, 89:940–956.

Hanson, G. J., and D. M. Temple. 2002. Performance of bare-earth and vegetated steep channels under long-duration flows. *Transactions of the American Society of Agricultural Engineers*, ASAE, 45(3):695–701.

Henderson, F. M. 1966. *Open channel flow*. New York: MacMillian Publishing Co.

Hughes, S. A. 2007. *Estimation of overtopping flow velocities on earthen levees due to irregular waves*. Coastal and Hydraulics Laboratory Engineering Technical Note ERDC/CHL CHETN-III-77. Vicksburg, MS: U.S. Army Engineer Research and Development Center.

_____. 2008. *Estimation of combined wave and storm surge overtopping at earthen levees*. Coastal and Hydraulics Laboratory Engineering Technical Note ERDC/CHL CHETN-III-78. Vicksburg, MS: U.S. Army Engineer Research and Development Center.

Independent Levee Investigation Team (ILIT). 2006. Investigation of the performance of the New Orleans flood protection systems in Hurricane Katrina on August 29, 2005. Volume I: Main Text and Executive Summary, Independent Levee Investigation Team. *http://www.ce.berkeley.edu/~new_orleans/report/VOL_1.pdf*

Munson, B. R., D. F. Young, and T. H. Okiishi. 1990. *Fundamentals of fluid mechanics*. 3rd Ed. New York: John Wiley & Sons, Inc.

Sturm, T. W. 2001. *Open channel hydraulics*. New York: McGraw-Hill Higher Education.

NOTE: *The contents of this technical note are not to be used for advertising, publication, or promotional purposes. Citation of trade names does not constitute an official endorsement or approval of the use of such products.*